Available online at www.sciencedirect.com
ScienceDirect
International Journal of Heat and Mass Transfer 51 (2008) 4470–4479
International Journal of HEAT and MASS TRANSFER
www.elsevier.com/locate/ijhmt

A theoretical study of the specific heat and Debye temperature of low-dimensional materials

Mei-Jiau Huang [a,*], Tai-Ming Chang [a], Chun-Kai Liu [b], Chih-Kuang Yu [b]

[a] Department of Mechanical Engineering, National Taiwan University, Taipei, Taiwan
[b] Electronics and Optoelectronics Research Laboratories, Industrial Technology Research Institute, Taipei, Taiwan

Received 22 March 2007; received in revised form 9 October 2007
Available online 8 April 2008

Abstract

A theoretical model is proposed in this work for an evaluation of the specific heat and Debye temperature of low-dimensional materials. In the model, the allowed discrete vibration modes in the confined direction(s) are first obtained by solving the elastic vibration equation. The acoustic specific heat is then calculated by summing over these discrete, excited, phonon modes and integrated over the continuous wave numbers in the unconfined directions. An effective Debye temperature is then defined as the one appearing in the conventional Debye model that gives a same value for the specific heat. It is found that the so-defined Debye temperature of the mixed polarization associated with nanowires is about half the longitudinal Debye temperature of bulk materials at room temperature. This agrees with the experimental observations. Those of both the dilatational and flexural polarizations associated with the thin films on the other hand are about 28% smaller than the bulk longitudinal Debye temperature. When the temperature is so low that there are only a few phonon modes excited, these low-dimensional materials show two-dimensional behavior, excluding the flexural polarization of the thin films, which shows one-dimensional behavior instead due to its parabolic dispersion relation at small dimensionless wave numbers.

Keywords: Acoustic specific heat; Effective Debye temperature; Phonon dispersion relation

1. Introduction

Low-dimensional materials such as nanowire and thin-film materials have attracted a lot of attention recently because they provide desirable thermal/electrical properties for possible improvements of IC thermal management, and also because remarkable advances in the fabrication technology nowadays have been made. For example, it is well known that the applications of a thermoelectric cooler are limited by its cooling efficiency, which in turn is limited by the material properties. The thermoelectric property of a material is usually characterized by its figure of merit, $Z = S^2\sigma/k$, where S is the Seebeck coefficient, σ is the electric conductivity, and k is the thermal conductivity [1]. The commonly known thermoelectric materials have ZT values between about 0.6 and 1.0 at room temperature $T = 300$ K. Recently, it has been found experimentally as well as theoretically [2–4] that low-dimensional materials such as quantum wells, quantum wires, quantum dots, and superlattice structures have ZT values much larger than their bulk counterparts. The increase in ZT values is attributed to the changed band structures, the modified dispersion relations, and the enhanced boundary scattering due to the size confinement effects [5–7].

In addition to the thermal and electric conductivities, the specific heat and the Debye temperature associated with these low-dimensional materials are also found different from the bulk values. Dames et al. [8] measured the phonon specific heat of the cold-pressed titanium dioxide nanotubes with typical dimensions of 500–1000 nm in length, 9 nm in outside diameter, and 2.5 nm in wall thickness. The temperature-dependence of the measured specific heat is found to shift from 3D to 2D behavior as the aver-

* Corresponding author. Tel.: +886 2 3366 2696; fax: +886 2 2363 1755.
E-mail address: mjhuang@ntu.edu.tw (M.-J. Huang).

0017-9310/$ - see front matter © 2008 Elsevier Ltd. All rights reserved.
doi:10.1016/j.ijheatmasstransfer.2008.02.007

age phonon mean free path becomes comparable to the wall thickness. A second transition from 2D to 1D behavior appears when the average phonon mean free path becomes comparable to the nanotube circumference. Neeleshwar et al. [9] investigated the size effect on magnetic susceptibility and heat capacity of CdSe quantum dots. A shrinkage of the lattice constants was observed. The magnitude of magnetic susceptibility is larger for smaller particles at all temperatures. And most of all, a Debye temperature that is really half the bulk value (139 K) is found based on the measurements of specific heats. Comsa et al. [10] measured the specific heats of Pd nanoparticles, compared to the predictions from a homogeneous elastic vibration theory. It was found that the sound speed employed in the theory must be adjusted in order to fit the measurements, resulting in much smaller Debye temperatures at low temperatures. A size dependence of the Debye temperature was actually also observed in many other metal nanoparticles [10].

Wang et al. [11] employed an elastic continuum model for fine nanoparticles to investigate theoretically the size effect on the specific heat, which counts contributions from interior as well as surface atoms. A dimensionless variable, inversely proportional to the sphere volume and the square of temperature, was proposed to characterize the effect of particle size and temperature. Prasher and Phelan [12,13] performed a similar analysis on thin solid films. An emphasis was put on the difference between discrete available phonon modes due to the thin film thickness and the integration approximation. It was found then the size effects are most important at cryogenic temperatures. The dimensionless parameter proposed for characterization is inversely proportional to temperature and film thickness. These analyses [11–13] nonetheless all adopted an approximate linear phonon dispersion relation, namely the Debye model or a constant phonon group velocity. As early as 1921, Schäfer [14] pointed out a discrete spectrum of eigenfrequencies exists due to the finite size. Baltes and Hilf [15] and Lautenschläger [16] employed such a discrete spectrum of scalar vibrations of metal spherical particles in calculating the heat capacity for lead grains. The existence of a peak in the specific heat enhancement was observed and explained. A weak size dependence of an "effective" Debye temperature was found as well.

Most of the previous work has been done for approximately spherical particles of the dimension on the order of a few nanometers and focused on the size dependence of the heat capacity. Few investigated nanowires and thin films. Moreover, a size dependence of the Debye temperature has also been noticed [8–10,16–18] and worth understanding. Recently, Yang et al. [19] induced the results of Lindemann's criterion [20] for melting, Mott's equation [21] and the Debye model. The size dependence of Debye temperatures of nanocrystals is obtained based on a size-dependent root of mean square amplitude model. Intricate models nonetheless are needed in order to distinguish the contributions of surface and interior atoms of nanocrystals. In the present paper, we instead aim at building a theoretical model that is capable of taking the size confinement effect directly into the calculations of the heat capacity of nanowires and thin films. Proper (effective) Debye temperatures suitable for nanocrystals will be defined and discussed. The size effect and temperature-dependence will be both explored. The rest of this paper is arranged as follows. The conventional Debye models for one-, two-, and three-dimensional (bulk) materials will be first reviewed in Section 2.1. The proposed models for nanowires and thin films are given in Section 2.2. The theoretical results of nanowires will be presented and discussed in Section 3. Followed are those of thin films in Section 4. Conclusions will be given at last in Section 5.

2. Mathematical models

2.1. Conventional Debye model

We first consider bulk crystalline solids which possess a linear phonon dispersion relation, $\omega = qV$, where ω, q, and V are the phonon frequency, wave number, and group velocity respectively. The phonon internal energy in the conventional i-dimensional ($i = 1$, 2, or 3) Debye model, under the integration approximation, is calculated as [22]

$$U_{i\mathrm{D}} = \frac{1}{(2\pi)^i} \cdot \int n_0 \hbar\omega \mathrm{d}\vec{q}_{i\mathrm{D}} \tag{1}$$

where n_0 is the Bose–Einstein distribution, namely

$$n_0(\omega, T) = (\exp(\hbar\omega/k_{\mathrm{B}}T) - 1)^{-1} \tag{2}$$

($\hbar$ and k_{B} are the Planck constant divided by 2π and the Boltzmann constant). By taking derivative with respective to temperature and employing the linear dispersion relation, one obtains the i-dimensional specific heat at constant volume for one polarization as follows:

$$C_{\mathrm{V,3D}} = \frac{k_{\mathrm{B}} q_{\max}^3}{6\pi^2} \cdot F_3\left(\frac{\theta_{\mathrm{D}}}{T}\right) \quad \text{(per unit volume)} \tag{3}$$

$$C_{\mathrm{V,2D}} = \frac{k_{\mathrm{B}} q_{\max}^2}{4\pi} \cdot F_2\left(\frac{\theta_{\mathrm{D}}}{T}\right) \quad \text{(per unit area)} \tag{4}$$

$$C_{\mathrm{V,1D}} = \frac{k_B q_{\max}}{\pi} \cdot F_1\left(\frac{\theta_{\mathrm{D}}}{T}\right) \quad \text{(per unit length)} \tag{5}$$

where $\theta_{\mathrm{D}} = \hbar\omega_{\max}/k_{\mathrm{B}}$ is the bulk Debye temperature, $\omega_{\max} = q_{\max}V$, and $q_{\max}$ is the maximum or cutoff wave number. The function $F_i(z)$ is defined as

$$F_i(z) = i \cdot z^{-i} \cdot \int_0^z \frac{x^{i+1}\mathrm{e}^x}{(\mathrm{e}^x - 1)^2}\mathrm{d}x \tag{6}$$

and is normalized by $F_i(0)$=1. Obviously F_i (and thus $C_{\mathrm{V},i\mathrm{D}}$) is approximately proportional to T^i at extremely low temperatures and this is characterized as the i-dimensional behavior. It must be mentioned herein although optical phonons also make contributions to specific heat, only acoustic phonons are considered in the present investigation and it is the acoustic specific heats that will be used

later to define the effective Debye temperatures of low-dimensional materials.

2.2. Low-dimensional Debye model

When low-dimensional materials such as films and nanowires are considered, the finite size effect generates a discrete phonon spectrum in the confined dimension(s). Infinitely many and discrete phonon vibration modes for a given plane (films) or axial (nanowires) wave component are thus resulted [23,24]. In this work, the size confinement effect is taken into consideration by adopting such confined dispersion relations. The integral approximation is nonetheless made in the unconfined directions. The phonon internal energy therefore becomes

$$U_{\text{wire}} = \sum_m \frac{1}{2\pi} \int n_0 \hbar\omega_m \mathrm{d}q_x \quad \text{(per unit length)} \tag{7}$$

for nanowires (q_x is the axial wave component) and

$$U_{\text{film}} = \sum_m \frac{1}{(2\pi)^2} \int (n_0 \hbar\omega_m) \times (2\pi q_{2\text{D}}) \mathrm{d}q_{2\text{D}} \quad \text{(per unit area)} \tag{8}$$

for films ($q_{2\text{D}}$ is the plane wave number), where the summation is done over the excited discrete modes in the confined direction(s). The specific heats are next obtained by taking derivatives of Eqs. (7) and (8) with respect to temperature T. The results can be arranged as follows

$$C_{\text{V,wire}} = \frac{k_{\text{B}}}{\pi a} \sum_m \int_0^{q_{\max} a} \times \frac{x_m^2 \mathrm{e}^{x_m}}{(\mathrm{e}^{x_m} - 1)^2} \mathrm{d}(q_x a) \quad \text{(per unit length)} \tag{9}$$

and

$$C_{\text{V,film}} = \frac{k_{\text{B}}}{2\pi a^2} \sum_m \int_0^{q_{\max} a} \frac{x_m^2 \mathrm{e}^{x_m}}{(\mathrm{e}^{x_m} - 1)^2} \times (q_{2\text{D}} a) d(q_{2\text{D}} a) \quad \text{(per unit area)} \tag{10}$$

where $x_m = \hbar\omega_m / k_{\text{B}} T$ is the dimensionless frequency of the mth excited phonon mode and a is the radius of the nanowires or the thickness of the thin films. As long as the discrete spectra of phonons are known, one can now compute the specific heats of nanowires and thin films according to the above two equations.

To define an "effective" Debye temperature for the low-dimensional materials, we first pretend that these low-dimensional materials, like their bulk counterparts, have a single linear phonon dispersion relation and that the integration approximation is applicable in all directions. Therefore Eqs. (7) and (8) can be further approximated as

$$U_{\text{wire}} \approx \frac{a}{(2\pi)^2} \cdot \int \int n_0 \hbar\omega \mathrm{d}q_x \mathrm{d}q_r \tag{11}$$

and

$$U_{\text{film}} \approx \frac{a}{(2\pi)^3} \cdot \int \int (n_0 \hbar\omega)(2\pi q_{2\text{D}}) \mathrm{d}q_{2\text{D}} \mathrm{d}q_z \tag{12}$$

In particular, because only axisymmetric phonon vibration modes in nanowires will be investigated later, the integration in Eq. (11) is performed over x and r directions only. By substituting the pretended linear phonon dispersion relation into Eqs. (11) and (12) and performing derivatives, one obtains

$$C_{\text{V,wire}} = \frac{k_{\text{B}} q_{\max}^2 a}{4\pi} \cdot F_2\left(\frac{\theta_{\text{D,wire}}}{T}\right) \quad \text{(per unit length)} \tag{13}$$

and

$$C_{\text{V,film}} = \frac{k_{\text{B}} q_{\max}^3 a}{6\pi^2} \cdot F_3\left(\frac{\theta_{\text{D,film}}}{T}\right) \quad \text{(per unit area)} \tag{14}$$

where $\theta_{\text{D,wire}}$ and $\theta_{\text{D,film}}$ are the Debye temperatures associated with the pretended linear dispersion relation. We are now ready to define the effective Debye temperatures of low-dimensional materials as follows. The specific heat is first computed based on Eqs. (9) and (10) and on the discrete phonon spectra. The parameter $\theta_{\text{D,wire}}$ or $\theta_{\text{D,film}}$ is then adjusted until Eqs. (13) or (14) is fitted to the computed specific heat. The resulting $\theta_{\text{D,wire}}$ or $\theta_{\text{D,film}}$ is hereafter defined as the desired effective Debye temperature.

3. Nanowires

3.1. Phonon spectrum

In this section, we attempt to investigate the size effect on the specific heat and Debye temperature of nanowires. The acoustic modes in an isotropic continuum material can be obtained by solving the lattice displacement equation,

$$\frac{\partial^2 u_i}{\partial t^2} = s_{\text{t}}^2 \nabla^2 u_i + (s_{\text{l}}^2 - s_{\text{t}}^2) \frac{\partial^2 u_j}{\partial x_i \partial x_j} \tag{15}$$

where u_i is the lattice displacement, and s_{l} and s_{t} are the bulk longitudinal and transverse sound speeds. In the case of circular nanowires, axisymmetric vibration modes have been reported [23,24]. Two polarizations are involved. One of them is purely transverse (with only azimuthal component of amplitude for waves propagating in the axial direction) and its dispersion relation is given by

$$J_0(q_\theta a) - \frac{2}{q_\theta a} J_1(q_\theta a) = 0 \tag{16a}$$

$$\omega^2 = s_{\text{t}}^2 (q_x^2 + q_\theta^2) \tag{16b}$$

The other one is a mixed mode of longitudinal and transverse polarizations. Its dispersion relation is determined by

$$4q_x^2q_l^2\frac{(q_ta)J_0(q_ta)}{J_1(q_ta)}-2q_l^2\ (q_x^2+q_t^2)+(q_x^2-q_t^2)^2\frac{(q_la)J_0(q_la)}{J_1(q_la)}=0 \tag{17a}$$

$$\omega^2=s_l^2(q_x^2+q_l^2)=s_t^2(q_x^2+q_t^2) \tag{17b}$$

where J_0 and J_1 are the Bessel functions of zeroth and first order. Both sets of equations, Eqs. (16ab) and (17ab), are suitable for free-stranding nanowires and have infinitely many and discrete solutions (q_l,q_t) for a given wave number q_x as illustrated in Fig. 1a and b for a silicon nanowire ($s_l = 8.47$ km/s, $s_t = 5.34$ km/, and $q_{max} = 11.4\ nm^{-1}$). As seen, the spectra are nonlinear, especially at smaller values of q_xa. It implies stronger size effect for finer wires. Moreover, the smaller the radius, the larger the energy gaps between adjacent modes for a given q_xa are and consequently the less important the higher modes are.

3.2. Specific heat and Debye temperature

Before we present the computational results of the specific heat based on Eq. (9) and the spectra in Fig. 1, attention must be paid to the fact that the number of discrete modes that can be excited is limited by the material size [12,13]. In the present study, it is determined in the following way. First, for a given wave number q_x, the number of allowed discrete modes is estimated to be

$$m(q_x)=\left[2\sqrt{q_{max}^2-q_x^2}/(2\pi/a)\right]+1 \tag{18}$$

where $[x]$ is the Gauss notation that gives the largest integer less than x. The number one in Eq. (18) counts the mode $q_r = 0$. The total number of allowed modes per unit length is therefore equal to

$$N_d=\frac{1}{2\pi}\int_{-q_{max}}^{q_{max}}m(q_x)dq_x \tag{19}$$

A detailed examination finds that N_d is slightly different from its continuous counterpart,

$$N_c=\frac{a}{(2\pi)^2}\int\int_{q_r^2+q_x^2\le q_{max}^2}dq_rdq_x=\frac{q_{max}^2a}{4\pi} \tag{20}$$

A correction factor $\varepsilon = N_c/N_d$ is therefore multiplied to $C_{V,wire}$ before it is substituted into Eq. (13) for searching the root $\theta_{D,wire}$. The factor is about 1.02 when $a = 10$ nm and approaches to one as the wire radius increases.

Shown in Fig. 2 is the so calculated specific heat for a silicone wire of diameter 20 nm. Note the specific heat has been divided by the cross-sectional area πa^2 and therefore has a unit of J/cm^3 K. It is seen the specific heat of the nanowire has a 2D behavior at intermediate temperatures but 1D behavior at very low temperatures. An examination shows when the temperature is very low, only the two lowest phonon modes are excited (or have significant phonon populations). The value of specific heat is mainly contributed by the first mode and slightly modified by the second one. This situation was also noticed by Baltes and Hilf [15]. The summation in Eq. (9) therefore plays no role, resulting in 1D behavior. Finally, the values of specific heat

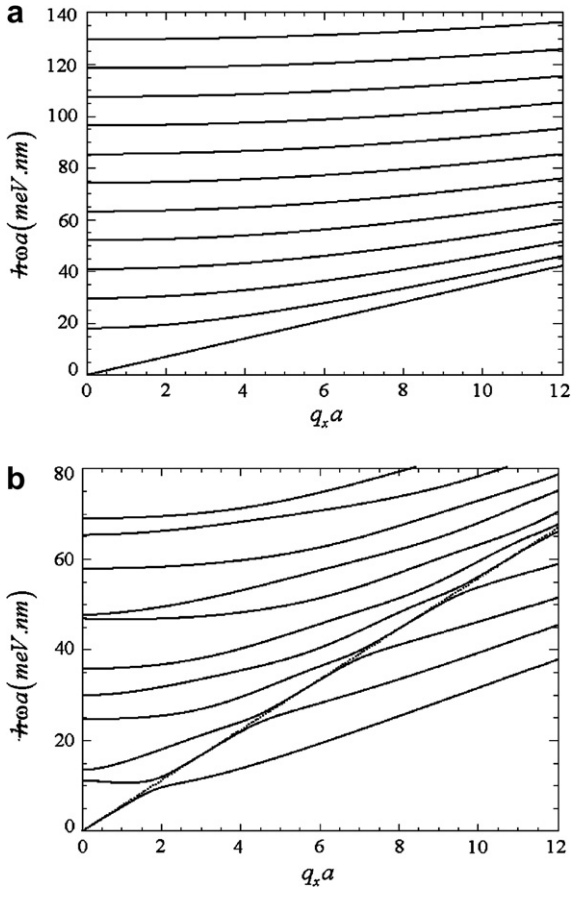

Fig. 1. The eigenmodes of the transverse polarization (a) and mixed polarization (b) of a silicon nanowire. The dotted line is the linear dispersion relation of the bulk longitudinal polarization (the constant group velocity is s_l).

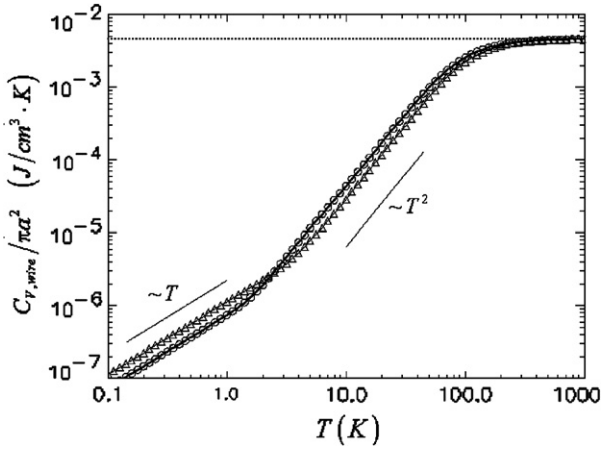

Fig. 2. The specific heat calculated based on Eq. (9) and the discrete phonon spectra for a silicon nanowire of diameter 20 nm. Symbols ○ and △ represent the mixed and transverse polarizations. The dotted line is the limiting value $k_Bq_{max}^2/4\pi^2a\varepsilon$.

approach to the limiting value, $k_B q_{max}^2/4\pi^2 a\varepsilon$, at high temperatures as expected.

The effective Debye temperature solved from Eq. (13) is shown in Fig. 3. It is seen that the effective Debye temperature is nearly constant at intermediate and high temperatures but drops like $T^{1/2}$ at low temperatures. Because the specific heat shows 1D behavior at low temperatures as seen in Fig. 2, we also try to fit the calculated specific heat by Eq. (5). The resulting Debye temperature is denoted as $\theta_{D,1D}$, and also shown in Fig. 3. As seen, the "1D effective Debye temperature" is nearly constant at low temperatures and drops like T^{-1} at high temperatures. The non-constancy of either $\theta_{D,wire}$ or $\theta_{D,1D}$ arises from the influence of the number of the phonon modes that can be excited at a given temperature and a given diameter, and implies neither one is suitable to the whole range of temperatures.

The transition of the specific heat from 1D to 2D behavior is observed for all wire radii investigated herein. The only difference is the temperature that the transition occurs decreases with increasing wire radius. This is because high modes contribute relatively less for finer wires as mentioned before. We thus define the transition temperature T_1 (T_2) as the temperature at which $\theta_{D,1D}$ ($\theta_{D,wire}$) has dropped to 99% of its asymptotic value as temperature increases (decreases). The size effects on the transition temperatures as well as on the asymptotic effective Debye temperatures are then shown in Figs. 4 and 5. It is seen the transition temperatures are inversely proportional to the wire radius. This is probably because the total number of available phonon modes is proportional to the wire radius as seen from Eq. (20). On the other hand, it is also found that the value of the specific heat (per unit volume) decreases with increasing wire radius. A further examination finds (see Fig. 6) that it is inversely proportional to the square of the wire radius at low temperatures (1D regime) and to the wire radius at intermediate temperatures (2D regime). The latter can be easily explained by Eq. (13) and the former must be understood from Eq. (5).

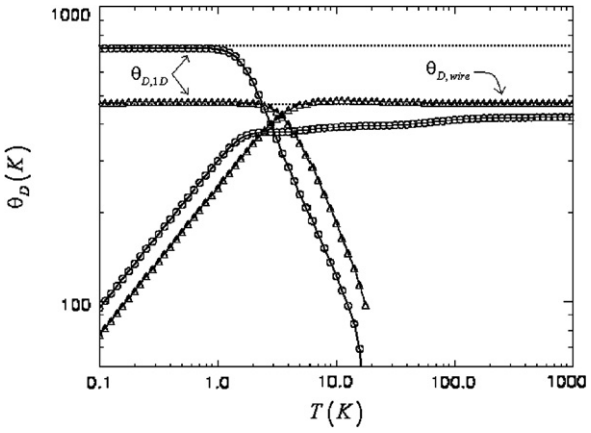

Fig. 3. The Debye temperatures obtained by solving Eqs. (5) and (13). The dotted lines are the bulk longitudinal and transverse Debye temperatures. Symbols ○ and △ represent the mixed and transverse polarizations.

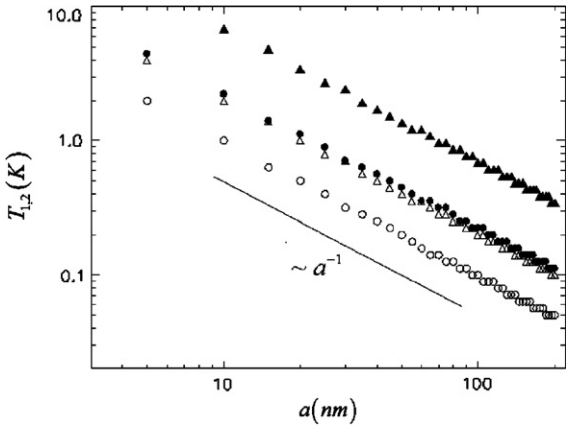

Fig. 4. The size effect on the transition temperatures. Symbols ○ and △ represent the mixed and transverse polarizations. Solid symbols are T_2 and open symbols are T_1.

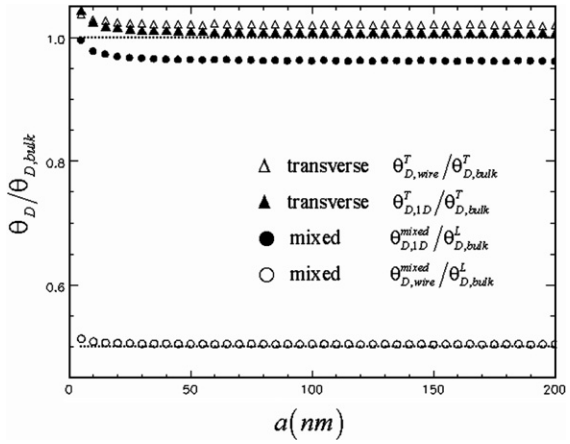

Fig. 5. The size effect on the asymptotic effective Debye temperatures normalized by the bulk longitudinal or transverse Debye temperature.

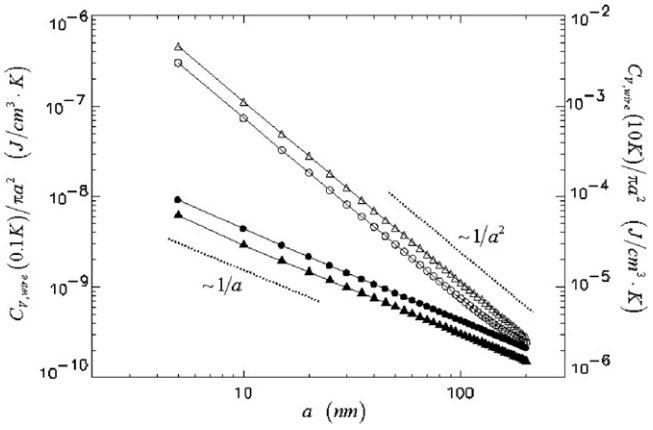

Fig. 6. The size dependence of the specific heats of the mixed (circle) and transverse (triangle) polarizations at $T = 0.1$ K (open symbols) and $T = 10$ K (solid symbols).

Finally, Fig. 5 shows the asymptotic effective Debye temperatures are nearly independent of the wire radius. The $\theta_{D,1D}$ of the mixed polarization is only slightly less

than the bulk longitudinal one ($\theta^{L}_{D,bulk} = 737.5$ K). This is because the first (lowest) phonon mode in Fig. 1b is dominant at low temperatures and has a group velocity close to bulk longitudinal sound speed (s_l) at small dimensionless wave numbers $q_x a$. The $\theta_{D,wire}$ of the mixed polarization nonetheless is only about half the bulk longitudinal Debye temperature. This is attributed to the influence of higher modes that have much smaller group velocities. In fact, a similar result is obtained when different values for s_l, s_t and q_{max} are used for different materials as long as these materials are made into nanowires. Although the titanim dioxide nanotubes investigated by Dames et al. [8] are hollow, they found a Debye temperature of 260 K, which is exactly half of the bulk counterpart (520 K), agreeing with the prediction herein. On the other hand, both $\theta_{D,1D}$ and $\theta_{D,wire}$ for the transverse polarization remain close to the bulk transverse Debye temperature ($\theta^{T}_{D,bulk} = 465$ K).

Finally, it must be emphasized again that in the present study only axisymmetric phonon modes are considered. In other words, the degree of freedom in the azimuthal direction is not taken into consideration. Therefore, if one considers the cases in which the mean free path of phonons is comparable to the wire radius but still much less than the circumference, i.e. the confinement effect in the azimuthal direction is not significant, the transition from 2D behavior to 1D behavior mentioned above should be actually a transition from 3D to 2D behavior, corresponding to the first transition observed by Dames et al. [8].

4. Thin films

4.1. Phonon spectrum

The confined phonon dispersion relation associated with thin films can be also obtained by solving Eq. (15). As far as free-standing thin films are concerned, the normal mode analysis [23] shows there are three possible polarizations - the shear waves, the dilatational waves, and the flexural waves. The dispersion relation of the transverse shear waves is determined by

$$\omega_n^2 = s_t^2(q_{z,n}^2 + q_{2D}^2) \tag{21}$$

where $q_{z,n} = n\pi/a$ is the quantized wave vector in the thickness (z)-direction and n is any integer. The dispersion relations for the other two mixed polarizations are

$$\omega^2 = s_l^2(q_l^2 + q_{2D}^2) = s_t^2(q_t^2 + q_{2D}^2) \tag{22a}$$

$$\frac{\tan(q_t a/2)}{\tan(q_l a/a)} = -\frac{4q_{2D}^2 q_l q_t}{(q_t^2 - q_{2D}^2)^2} \tag{22b}$$

for the dilatational waves, and

$$\omega^2 = s_l^2(q_l^2 + q_{2D}^2) = s_t^2(q_t^2 + q_{2D}^2) \tag{23a}$$

$$\frac{\tan(q_l a/2)}{\tan(q_t a/2)} = -\frac{4q_{2D}^2 q_l q_t}{(q_t^2 - q_{2D}^2)^2} \tag{23b}$$

for the flexural waves. Solutions of Eqs. (21), (22ab), and (23ab) are all infinitely many and discrete as illustrated by silicon thin films in Fig. 7a–c. The first mode of dilatational (shear) waves has a group velocity close to the bulk longitudinal (transverse) sound speed at small dimensionless wave numbers, $q_{2D}a$. The group velocity of the flexural waves nonetheless vanishes at $q_{2D} = 0$ (Fig. 7c). The dispersion relation is actually parabolic near the origin. For all three polarizations, the larger the thickness of the film, the smaller the energy gaps between adjacent modes for a given $q_{2D}a$ are.

4.2. Specific heat and Debye temperature

Similar to the nanowire cases, a correction factor ε is also needed in the thin-film cases to compensate the difference between the discreteness and the continuity. For a given plane wave number q_{2D}, the number of allowed discrete modes is

$$m(q_{2D}) = \left[2\sqrt{q_{max}^2 - q_{2D}^2}/(2\pi/a)\right] + 1 \tag{24}$$

and the total number per unit area is

$$N_d = \frac{1}{(2\pi)^2}\int_0^{q_{max}} m(q_{2D})(2\pi q_{2D})\mathrm{d}q_{2D} \tag{25}$$

The continuous one on the other hand is

$$N_c = \frac{a}{(2\pi)^3}\cdot\frac{4\pi}{3}q_{max}^3 \tag{26}$$

The correction factor $\varepsilon = N_c/N_d$ is about 0.99 when the film thickness is 20 nm and it approaches gradually to one as the film thickness increases.

Fig. 8 shows the specific heats of a silicon thin film of thickness 10 nm. All polarizations show 3D behavior at temperatures approximately beyond 10 K, and have values of specific heats close to the limiting one ($k_B q_{max}^3/6\pi^2\varepsilon$) at high temperatures. At low temperatures, both dilatational and shear waves show 2D behavior. The transition arises again from the fact that only a few phonon modes are excited at such low temperatures and consequently the summation in Eq. (10) becomes functionless. The specific heat of the flexural waves, nonetheless, is linearly dependent on the temperature (1D behavior) at low temperatures. As mentioned before, the first mode of the flexural waves has a parabolic, instead of linear, dispersion relation at small dimensionless wave numbers (Fig. 7c). This causes a reduction by one in the power index of the temperature-dependence of specific heat. The one-dimensional behavior is therefore resulted. The total specific heat (a sum of specific heats of all three polarizations) is presented and compared with the bulk counterpart in Fig. 9. The deviation is obvious at low temperatures where size effect is strong. At last, it is also found (not shown herein) the specific heats per unit volume of all polarization are almost independent of the film thickness at high temperatures as suggested by

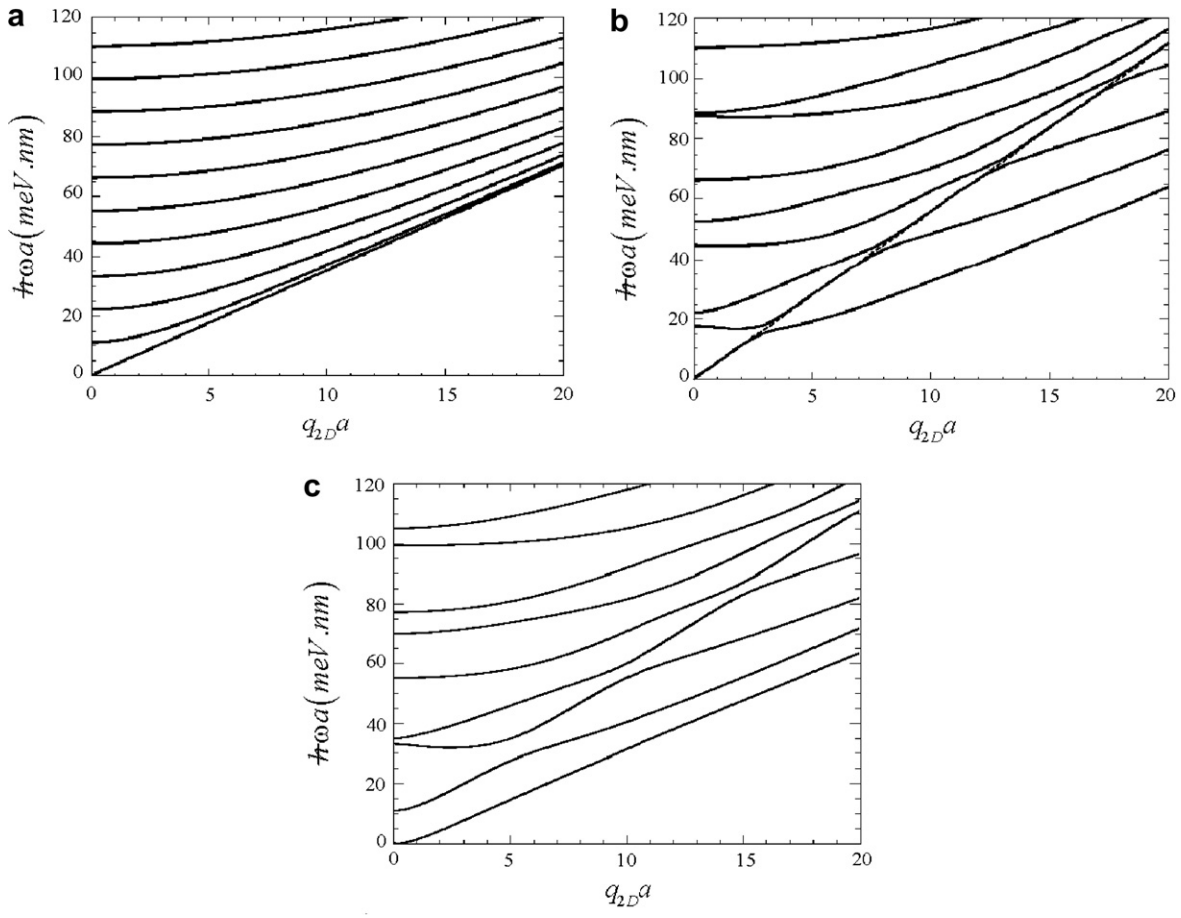

Fig. 7. The eigenmodes of the shear waves (a), the dilatational waves (b), and the flexural waves (c) of a silicon thin film.

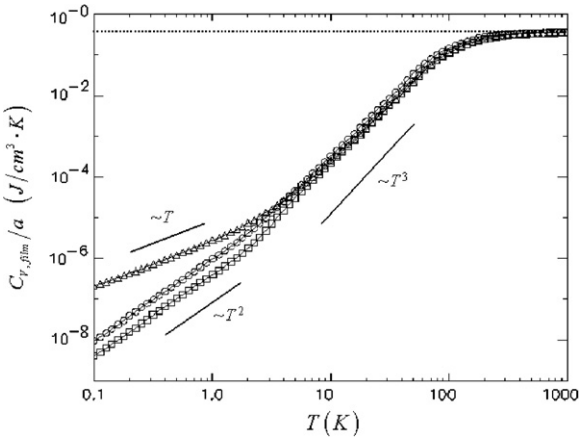

Fig. 8. The specific heat calculated based on Eq. (10) and the discrete spectra for a silicon thin film of thickness 10 nm. Symbols □, △, and ○ represent the dilatational, flexural, and shear waves, respectively. The dotted line is the limiting value $k_B q_{max}^3/6\pi^2\varepsilon$.

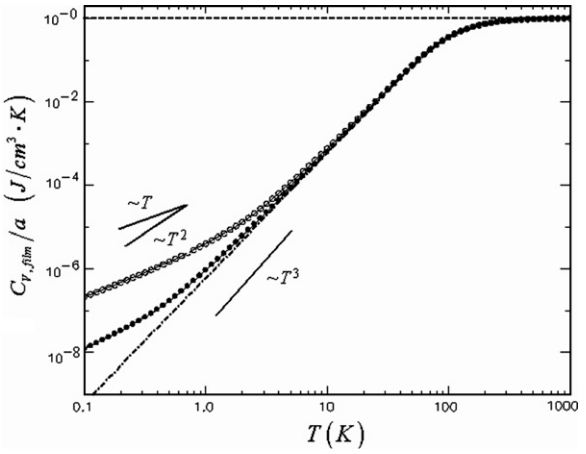

Fig. 9. The total specific heat of all three polarizations for silicon thin films of thickness 10 nm (open symbols) and 50 nm (solid symbols). The dash dotted line is the bulk result.

Eq. (14). The size dependences of them at low temperatures are nonetheless different. The specific heats of the dilatational and shear waves are inversely proportional to the film thickness while that of the flexural waves is inversely proportional to the square of the film thickness. The former is easily seen from Eq. (4). The latter can be explained by performing the integration in Eq. (10) under the assumption of a parabolic phonon dispersion relation $(\omega a) = c(q_{2D}a)^2$, where c is some constant. These size dependences are illustrated in Fig. 10, in which the specific heat against the film thickness at 0.1 K is presented.

Shown in Fig. 11 are the effective Debye temperatures solved from Eq. (14). It is seen all three effective Debye

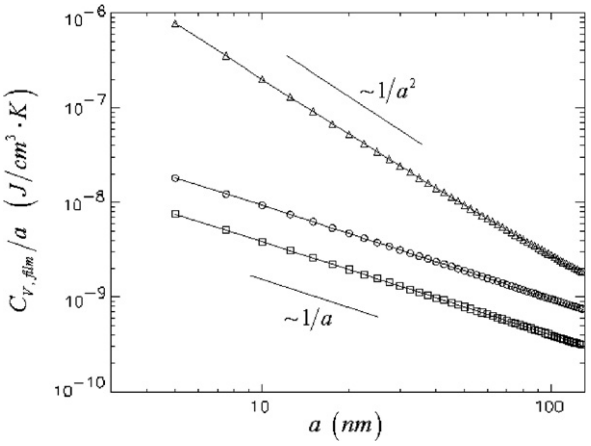

Fig. 10. The size dependence of the specific heats of dilatational (□), flexural (△), and shear (○) waves at 0.1 K.

temperatures are nearly constant beyond 100 K, but drop quickly at low temperatures. To better describe the low-temperature behavior, a "2D Debye temperature", denoted by $\theta_{D,2D}$, is defined in a similar way by taking advantage of Eq. (4) for shear as well as dilatational waves. The results are also shown in Fig. 11a and b. Without surprise, the "2D Debye temperatures" of dilatational and shear waves remain nearly constant at low temperatures and agree with $\theta^{L}_{D,bulk}$ and $\theta^{T}_{D,bulk}$ respectively. They decrease with increasing temperature at intermediate temperatures nonetheless. The power index associated with this decrease is close to $-5/12$. Because the flexural waves do not possess such 2D behavior, there exists no corresponding 2D Debye temperature in Fig. 11c.

To define the transition temperatures T_1 and T_2, we notice the oscillations appearing in the effective Debye temperature of the dilatational waves. We thus in this subsection define T_2 associated with the dilatational waves as the temperature where the local maximum of $\theta_{D,film}$ appears. The size dependence of the transition temperatures is then shown in Fig. 12. They are seen both inversely proportional to the film thickness, similar to those observed in nanowire cases.

The asymptotic values of the effective and 2D Debye temperatures against the film thickness are shown in Fig. 13. The Debye temperatures associated with the shear waves show little difference from the bulk transverse one. However, the effective Debye temperatures of the mixed polarizations are about 28% less than the bulk longitudinal Debye temperature.

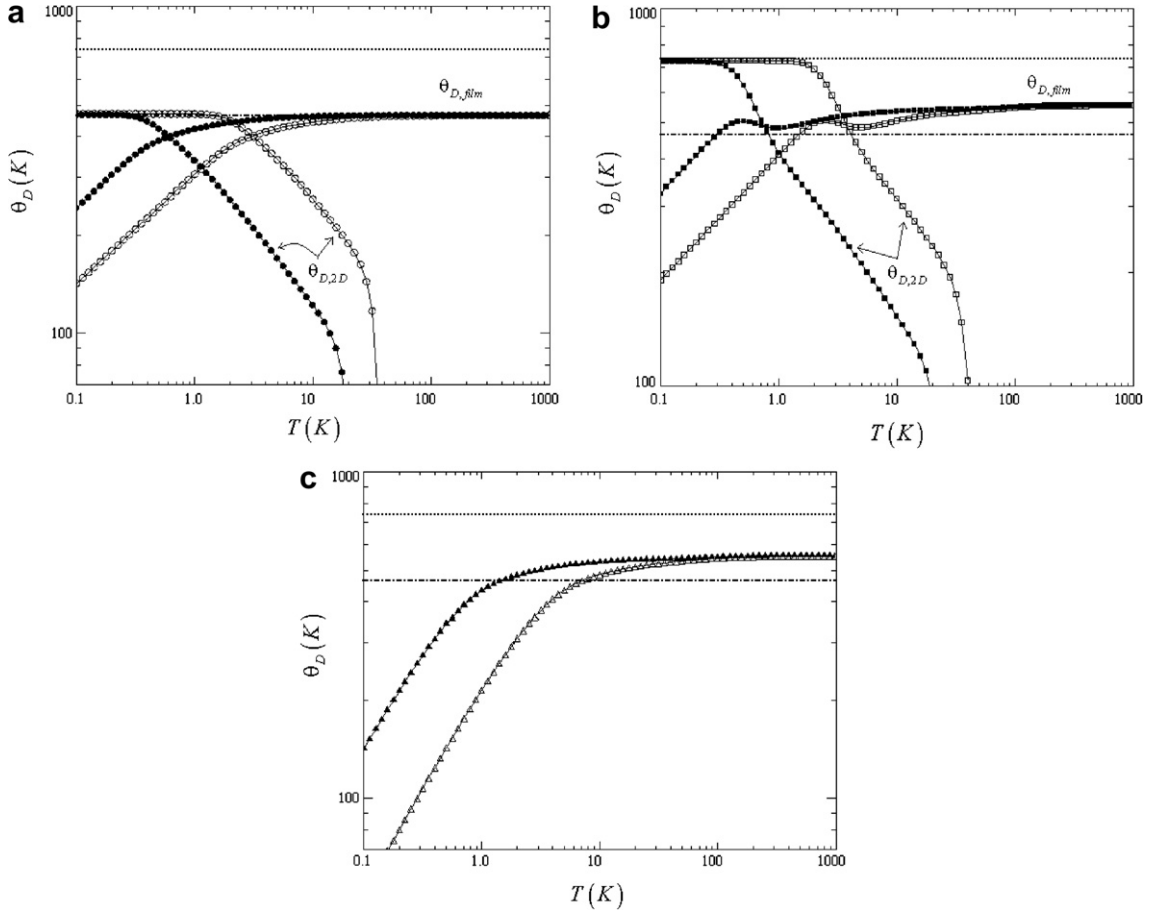

Fig. 11. The effective Debye temperature associated with the shear waves (a), the dilatational waves (b), and the flexural waves (c) of a silicon thin film of thickness 10 nm (open symbols) and 50 nm (solid symbols). The dotted and dotted dash lines indicate the bulk longitudinal and transverse Debye temperatures.

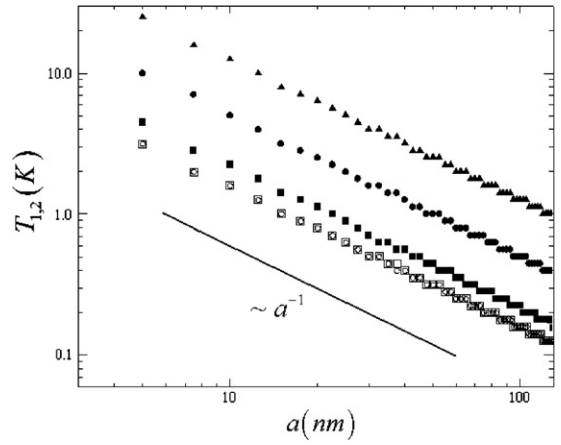

Fig. 12. The transition temperatures against the film thickness. Symbols □, △, and ○ represent the dilatational, flexural, and shear waves, respectively. Solid symbols are T_2 and open symbols are T_1.

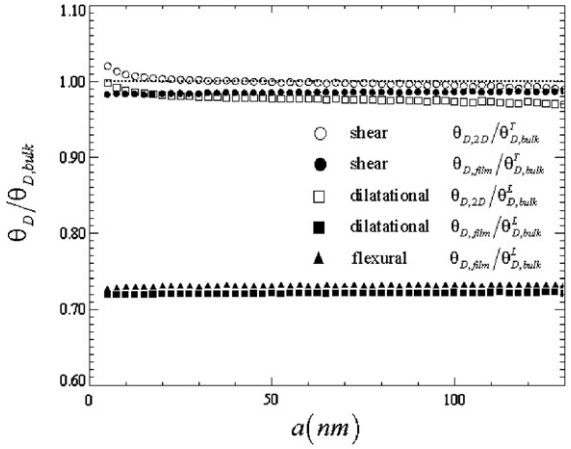

Fig. 13. The effective and 2D Debye temperatures against the film thickness.

5. Conclusions

A theoretical model is proposed in the present work in order to define a proper effective Debye temperature for low-dimensional materials under the size confinement effect. The specific heat is first evaluated based on the confined phonon dispersion relation, which is discrete in the confined dimension(s) and continuous in the others. In order to predict a same value for the specific heat by the conventional Debye model, it is found the associated Debye temperature must be adjusted and consequently is different from the bulk counterpart. The resulting Debye temperature is thus defined as the effective Debye temperature of the low-dimensional material under investigation.

The investigation shows the effective Debye temperature of the mixed polarization associated with nanowires is about half the longitudinal Debye temperature of bulk materials at intermediate temperatures. The agreement with the experimental observations [8] suggests maybe that the measured Debye temperature is that of the mixed polarization, instead of the bulk one, due to the small size of the specimens. The effective Debye temperatures of the mixed polarizations associated with thin films on the other hand are about 28% less than the bulk longitudinal Debye temperature. In the labs, the measured Debye temperature of thin films is also not much different from the bulk one [12]. At last, when the temperature is so low that there are only several phonon modes excited, the low-dimensional materials show two-dimensional behavior instead, excluding the flexural polarization of the thin films (which possesses one-dimensional behavior because of its parabolic dispersion relation at small dimensionless wave numbers).

Acknowledgement

The support of this work by the National Science Council, Taiwan, ROC under contract NSC 95-2221-E-002-336-MY2 and that by ITRI under the contract 3000138575 are gratefully acknowledged. Those valuable discussions with Prof. Juhn-Jong Lin from National Chiao-Tung University, Taiwan are highly appreciated.

References

[1] S. Wisniewski, B. Staniszewski, R. Szymanik, Thermodynamics of Nonequilibrium Processes, PWN-Polish Scientific Publishers, Boston, 1976.
[2] W.S. Capinski, M. Cardona, D.S. Katzer, H.J. Maris, K. Ploog, T. Ruf, Thermal conductivity of GaAs/AlAs superlattices, Physica B 263–264 (1999) 530–532.
[3] D.G. Cahilla, W.K. Ford, K.E. Goodson, G.D. Mahan, A. Majumdar, H.J. Maris, R. Merlin, S.R. Phillpot, Nanoscale thermal transport, J. Appl. Phys. 93 (2003) 793–818.
[4] R. Venkatasubramanian, E. Siivola, T. Colpitts, B. O'Quinn, Thin-film thermoelectric devices with high room-temperature Figures of merit, Nature 413 (2001) 597–602.
[5] G. Chen, A. Shakouri, Heat transfer in nanostructures for solid-state energy conversion, J. Heat Transfer 124 (2002) 242–252.
[6] J. Zou, A. Balandin, Phonon heat conduction in a semiconductor nanowire, J. Appl. Phys. 89 (2001) 2932–2938.
[7] A. Balandin, K.L. Wang, Significant decrease of the lattice thermal conductivity due to phonon confinement in a free-standing semiconductor quantum well, Phys. Rev. B 58 (1998) 1544–1549.
[8] C. Dames, B. Poudel, W.Z. Wang, J.Y. Huang, Z.F. Ren, Y. Sun, J.I. Oh, C. Opeil, M.J. Naughton, G. Chen, Low-dimensional phonon specific heat of titanium dioxide nanotubes, Appl. Phys. Lett. 87 (2005) 031901.
[9] S. Neeleshwar, C.L. Chen, C.B. Tsai, Y.Y. Chen, Size-dependent properties of CdSe quantum dots, Phys. Rev. B 71 (2005) 201307.
[10] G.H. Comsa, D. Heitkamp, H.S. Rade, Effect of size on the vibration specific heat of ultrafine palladium particles, Solid State Commun. 24 (1977) 547–550.
[11] B.X. Wang, L.P. Zhou, X.F. Peng, Surface and size effects on the specific heat capacity of nanoparticles, Int. J. Thermophys. 27 (2006) 139–151.
[12] R.S. Prasher, P.E. Phelan, Size effects on the thermodynamic properties of thin solid films, J. Heat Transfer 120 (1998) 1078–1081.
[13] R.S. Prasher, P.E. Phelan, Non-dimensional size effects on the thermodynamic properties of solids, Int. J. Heat Mass Transfer 42 (1999) 1991–2001.
[14] C. Schaefer, Einfuehrung in die theoretische Physik, Z. Phys. 7 (1921) 287.

[15] H.P. Baltes, E.F. Hilf, Specific heat of lead grains, Solid State Commun. 12 (1973) 369–373.
[16] R. Lautenschläger, Improved theory of the vibrational specific heat of lead grains, Solid State Commun. 16 (1975) 1331–1334.
[17] M.J. Huang, W.Y. Chong, T.M. Chang, The lattice thermal conductivity of a semiconductor nanowire, J. Appl. Phys. 99 (2006) 114318.
[18] M.J. Huang, T.M. Chang, W.Y. Chong, A new lattice thermal conductivity model of a thin film semiconductor, Int. J. Heat Mass Transfer 50 (2007) 67–74.
[19] C.C. Yang, M.X. Xiao, W. Li, Q. Jiang, Size effects on Debye temperature, Einstein temperature, and volume thermal expansion coefficient of nanocrystals, Solid State Commun. 139 (2006) 148–152.
[20] F.A. Lindemann, über die Berechnung Molecularer Eigenfrequenzen, Z. Phys. 11 (1910) 609–612.
[21] N.F. Mott, The resistance of liquid metals, Proc. R. Soc. London A 146 (1934) 465–472.
[22] N.W. Ashcroft, N.D. Mermin, Solid State Physics, Brooks/Cole, USA, 1976.
[23] N. Bannov, V. Aristov, V. Mitin, Electron relaxation times due to the deformation-potential interaction of electrons with confined acoustic phonons in a free-standing quantum well, Phys. Rev. B. 51 (1995) 9930–9942.
[24] A. Khitun, A. Balandin, K.L. Wang, Modification of the lattice thermal conductivity in silicon quantum wires due to spatial confinement of acoustic phonons, Superlattice Microst. 26 (1999) 181–193.